# Electron Tunneling in Proteins: Implementation of ZINDO Model for Tunneling Currents Calculations

**Xuehe Zheng and Alexei A. Stuchebrukhov***

*Department of Chemistry, University of California, Davis, California 95616*

*Received: October 8, 2002; In Final Form: April 21, 2003*

The tunneling currents method developed previously by this group for the description of electron tunneling in proteins and other complex molecular structures is implemented at the semiempirical ZINDO level. This implementation bridges the gap between fully ab initio and simple one electron methods, such as the extended Hückel method, which has been previously employed in tunneling studies, and allows for accurate calculations to be performed on realistic large protein systems with only a moderate effort. One additional advantage of this method is that it employs the STO basis functions, which decay more slowly than do GTO functions, so that the weak tunneling interactions of noncovalently bonded atoms of the protein can be accounted for with a minimum basis set. Numerical results are demonstrated on the polypeptide chain $(His)_2(Met)Cu^{1+}$-(Cys)-$(Gly_5)$-$(His)Ru^{3+}(bpy_2)Im$, which models the Ru-modified azurin charge transfer system studied by Gray and co-workers.

## 1. Introduction

Long-distance electron tunneling in complex molecular structures, such as proteins,[1−3] DNA,[4−6] and molecular wires,[7] has been a subject of active theoretical and computational research in the past decade. Several reviews of the topic have appeared recently, e.g., in refs 8−15. For large systems, such as proteins, the main computational challenge has been to evaluate accurately and efficiently the small electronic couplings between redox sites, which typically contain transition metal complexes and are separated by distances of 10−30 Å. These couplings are mediated by the protein medium. Another issue in proteins has been the mapping of tunneling pathways.[8−10,15]

The method of tunneling currents addresses both the pathways and the coupling issues within the same formalism.[15−17] The method has been implemented initially at one electron theory level and then extended to the many electron description. At present, for large protein systems, the calculations have been routinely done employing one electron extended Hückel theory,[18−20] and for reduced molecular models, obtained for example with the method of protein pruning,[21] the calculations have been carried out at the Hartree−Fock level[22] and with the use of density functional theory (DFT).[23]

This paper discusses the implementation of the method of tunneling currents using the many electron semiempirical intermediate neglect of differential overlap (INDO) model[24] for electron description of the protein medium. Specifically, we employ a widely used Zerner's version of the INDO model Hamiltonian originally developed for electronic spectroscopy.[25,26] This development bridges the gap between crude but efficient one electron methods and accurate but demanding fully ab initio methods. In the spirit of ZINDO approach, this implementation is both efficient and accurate and thus is particularly suitable for studies involving large biological systems. One additional advantage of this method is that it employs the STO basis functions, which decay with distance more slowly than do GTO functions, so that the weak tunneling interactions of noncovalently bonded atoms of the protein can be accounted for with a minimum basis set. The idea to use STO in the tunneling currents calculation was suggested to us by the late M. C. Zerner. (Of course, the exponential decay of the STOs does not in itself guarantee greater accuracy of calculations, because the empirical decay constants of STOs may not exactly correspond to the local barrier heights for electronic tunneling. The latter depends, among other things, on the type of atoms involved and their mutual distances. The hope, however, is that the empirical decay constants of STO in ZINDO are close enough to realistic values for organic materials, such as proteins, and will be of value for tunneling calculations; see the related discussion in ref 27. The exploration of such issues is one of the goals of the reported work.) Numerical results will be demonstrated on the polypeptide chain $(His)_2$-$(Met)Cu^{1+}$-(Cys)-$(Gly_5)$-$(His)Ru^{3+}(bpy_2)Im$, which models the Ru-modified azurin charge transfer system studied by Gray and co-workers.

In the past, the ZINDO model has been shown to be well-suited for treatment of sizable biological systems such as heme sites,[28] photosynthetic reaction centers in bacteria,[29,30] and light-harvesting antenna aggregates.[31] Newton[11−13,32] and Cave[33−35] have extensively used ZINDO for calculations of electronic couplings for electron transfer in a variety of inorganic or organic systems. This work demonstrates that the ZINDO model is both accurate and efficient when employed for tunneling currents calculations and can be utilized in studies of electron tunneling in large biological systems.

The plan of this paper is as follows: section 2 summarizes the theoretical framework of both electron tunneling and ZINDO model; section 3 gives numerical results that demonstrate the performance of the ZINDO implementation in tunneling calculations; and finally, the concluding remarks are made in section 4.

## 2. Tunneling Currents

A detailed discussion of the tunneling currents method can be found in a recent review.[15] The general idea of the approach is to examine dynamics of charge redistribution in a system that is artificially "clamped" at the transition state, when donor and acceptor states are degenerate.[36] To find the transition state,

10.1021/jp022203a CCC: $25.00 
Published on Web 06/17/2003

one may use external charges to mimic the fluctuating electric field within the protein, as described below in the text (see also refs 11 and 22). These fields shift redox potentials of donor and acceptor complexes and bring them occasionally to resonance, at which point electron tunneling occurs. One needs to keep in mind that the transition state of ET, i.e., the resonance condition, is not unique, and the details of the tunneling process can have significant variations.[22,37,38] The discussion of this point can be found elsewhere;[15] here, we will focus on describing tunneling in one possible resonant configuration of the ET system.

The tunneling dynamics is described by the following time-dependent wave function:

$$|\Psi(t)\rangle = \cos(T_{DA}t/\hbar)\,|D\rangle - i\,\sin(T_{DA}t/\hbar)\,|A\rangle \qquad (1)$$

where $|D\rangle$ and $|A\rangle$ are diabatic donor and acceptor states and $T_{DA}$ is the transfer matrix element. The diabatic states are localized on their respective complexes, but their exponentially small tunneling tails extend over the whole protein. In both one and many electron formulations of the problem, the time dependence of the wave function is the same. The periodic change of the wave function from donor to acceptor state results in periodic variations of charge distribution in the system. The redistribution of charge is associated with current. It is this tunneling current that we are focusing on in this method.

The redistribution of charge in the system during the tunneling transition can be described in terms of current density $\vec{j}(r, t)$ and its spatial distribution $\vec{J}(r)$.[16,17] The appropriate expressions for these quantities are obtained from the continuity equation

$$\frac{\partial\hat{\rho}}{\partial t} = -div\hat{j} \qquad (2)$$

which, when applied for the tunneling state, eq 1, yields

$$\vec{j}(\vec{r}, t) = -\vec{J}(\vec{r})\,\sin\frac{2T_{DA}t}{\hbar},\ \ \vec{J}(\vec{r}) = -i\,\langle A|\,\hat{j}(\vec{r})\,|D\rangle \qquad (3)$$

As expected, the periodic variation of charge distribution is associated with periodic time-dependent current, $\vec{j}(\vec{r}, t)$. The spatial distribution of current $\vec{J}(\vec{r})$, however, remains the same during the dynamic process. Given also the form of $\vec{J}(\vec{r})$, one concludes that $\vec{J}(\vec{r})$ is not related to specific periodic time dependence of the wave function eq 1 but rather is a more general characteristic of the quantum transition between states $|D\rangle$ and $|A\rangle$.

The tunneling current $\vec{J}(\vec{r})$ turns out to be related to the tunneling matrix element as follows:[17]

$$T_{DA} = -\hbar\int_{\partial\Omega_D}(d\vec{s}\cdot\vec{J}) \qquad (4)$$

In the above formula, $\Omega_D$ is the volume of space that comprises the donor complex, and $\partial\Omega_D$ is its surface. This relation is obtained using the conservation of charge argument.[17]

When computing tunneling matrix elements, the most significant problem is that the diabatic states, by their nature, are well-defined only in the regions of the localization of the charge, and perhaps in the tunneling barrier, but not in the far region of the other site. As a result, when matrix elements such as $\langle A|\,H\,|D\rangle$ over states $|D\rangle$ and $|A\rangle$ is evaluated, in the volume integral, there are major regions (around donor and acceptor) where one function is well-defined, but the other is not. This can potentially lead to numerical errors. In the method of tunneling currents, the calculation includes the region of the barrier only, where both functions $|D\rangle$ and $|A\rangle$ are well-defined.

The above formulation of the rate of tunneling transition is qualitatively similar to that of the transition state theory,[39] where the rate of the reaction is calculated using flux−flux correlation functions at the dividing surface that separates reactants and products in the phase space. As in the variational transition state theory,[40] in our case, the position of the dividing surface can also be adjusted to find the maximum flux and to avoid the "recrossings" of the reacting trajectories.

At the unrestricted HF level, the donor and acceptor states are taken to be single Slater determinants

$$|D\rangle = |\varphi^D_{1\alpha}\cdots\varphi^D_{p\alpha}\,\varphi^D_{1\beta}\cdots\varphi^D_{q\beta}\rangle \qquad (5)$$

$$|A\rangle = |\varphi^A_{1\alpha}\cdots\varphi^A_{p\alpha}\varphi^A_{1\beta}\cdots\varphi^A_{q\beta}\rangle \qquad (6)$$

To calculate the current density, one needs to evaluate the matrix element of the current operator over these two states. The calculations are convenient to carry out, however, not with these canonical HF states but with ones that are obtained with a certain orthogonal transformation of both states. Below, we describe briefly this so-called biorthogonalization procedure.

In general, the two sets of $\alpha$ and $\beta$ MOs are not orthogonal within its own spin parity (i.e., $\langle\varphi^D_i|\varphi^A_j\rangle \neq \delta_{ij}s_j$). However, as a special case of the mirror theorem,[41,42] by appropriate rotations of the canonical MOs of both states in the Hilbert space, the states $|A\rangle$ and $|D\rangle$ can be made pairwise orthogonal or biorthogonal.[43−45] In this case, the overlap matrix of states $|A\rangle$ and $|D\rangle$ becomes diagonal

$$\langle\varphi^A_{i\sigma}|\varphi^D_{j\sigma}\rangle = \delta_{ij}s^\sigma_i \qquad (7)$$

This transformation leads to a natural pairing of the MOs, which are sometimes called the corresponding orbitals of Amos and Hall[46] or the paired orbitals of Löwdin.[47] Such orbitals have been utilized in ET problems by Newton,[11] Friesner,[48] Goddard,[45] and their co-workers in the past to evaluate the Hamiltonian matrix element $\langle A|\,H\,|D\rangle$. The pairing of the orbitals leads to a crucial physical insight into how one can think about the tunneling in the many electron system (at least in the HF description). It turns out that only one pair of the corresponding orbitals contribute significantly to tunneling transition, the rest participate as an electronic Franck−Condon factor, as described below.

Suppose that $|D\rangle$ and $|A\rangle$ are such two biorthogonalized states; with $p$ orbitals in $\alpha$-spin and $q$ orbitals in $\beta$-spin, the expression for currents has the following form

$$\vec{J}(\vec{x}) = \frac{-\hbar}{2m}\det(\mathbf{S}_{AD})\sum_{i,\sigma}\frac{1}{s^\sigma_i}(\varphi^A_{i\sigma}(\vec{x})\nabla\varphi^D_{i\sigma}(\vec{x}) - \varphi^D_{i\sigma}(\vec{x})\nabla\varphi^A_{i\sigma}(\vec{x})) \qquad (8)$$

where

$$det(\mathbf{S}_{AD}) = \prod_i^p s^\alpha_i \prod_j^q s^\beta_j \qquad (9)$$

The total current in the system is given as a sum of contributions from corresponding orbitals of donor and acceptor states.

This expression is a generalization of the one electron picture. Now, different pairs of corresponding (overlapping) orbitals of donor and acceptor states contribute to the current density. The smaller the overlap between corresponding orbitals in donor and acceptor wave functions (i.e., the greater the change of an orbital

between the $|D\rangle$ and the $|A\rangle$ states), the greater the contribution of a given pair of orbitals to the current.

The total current in the above expression is a sum of the current due to tunneling charge per se and to polarization effects. In the Hartree−Fock approach, all electrons in the systems are treated on an equal footing; therefore, the expressions for both tunneling and polarization currents are similar in structure. The major contribution to the current, however, is due to one particular pair of external orbitals, which describe the tunneling electron. The orbitals of other ("core") electrons just shift slightly, due to polarization effects. Their contribution enters as an electronic Franck−Condon factor[11,32,49] in the expression for the tunneling electron current.

In practice, the currents are calculated in terms of some suitable atomic basis functions. The molecular orbitals $\varphi$'s are found as linear combinations of these functions, then the states are biorthogonalized, and the tunneling currents are calculated according to final formulas given in ref 15.

**2.1. Calculation of Donor and Acceptor States.** The tunneling calculations described above require the knowledge of two diabatic states—the initial donor state $|D\rangle$ and the final acceptor state $|A\rangle$. In two separate calculations, the transferred electron is localized on the donor and acceptor sites, respectively (the method of localization is described below), and the two states are calculated at the Hartree−Fock level using ZINDO model Hamiltonian. In these calculations, we use the standard parametrization described in ref 50. The sensitivity of the model parameters on the results is discussed later in the paper.

For an arbitrary nuclear configuration of the system, the donor and acceptor states will have different energies; therefore, the electron is localized in one of these states with the lowest energy. The transition state of an electron transfer reaction occurs when in the course of thermal fluctuations of the polar medium or charges surrounding donor and acceptor complexes, the two states reach a resonance.[36] To simulate such a resonance, an electric field or point charge is introduced in the computation to mimic the action of the environment.

The calculations proceed as follows. Suppose a point charge $Q$ is introduced along the line connecting donor and acceptor sites, some distance $l$ off the donor site. The charge $Q$ is such that it is strong enough to change energetics of the system and induce the electron transfer and yet small enough to leave the electronic structure of donor and acceptor states unaltered. The energies of the donor and acceptor electronic states roughly are

$$E_d = E_{d0} + Q\left(\frac{q_d}{l} + \frac{q_a}{R+l}\right) \tag{10}$$

$$E_a = E_{a0} + Q\left(\frac{q_d + 1}{l} + \frac{q_a - 1}{R+l}\right) \tag{11}$$

where $q_a$ and $q_d$ are charges on donor and acceptor complexes. It is then possible to tune the point charge $Q$ so as to make the two energies $E_d$ and $E_a$ to be as much as possible close to each other. Given the effort (for a large system) needed to obtain the two states for a given charge $Q$, in practice only, few such calculations are performed and series of data points $E_d(Q_i)$, $E_a(Q_j)$ are generated. The charge $Q\dagger$ at which the crossing of two curves occurs

$$E_d(Q\dagger) = E_a(Q\dagger) \tag{12}$$

is obtained by a linear (or similar) extrapolation of the region where the two energies are close to each other. These calculations are illustrated by Figure 1.

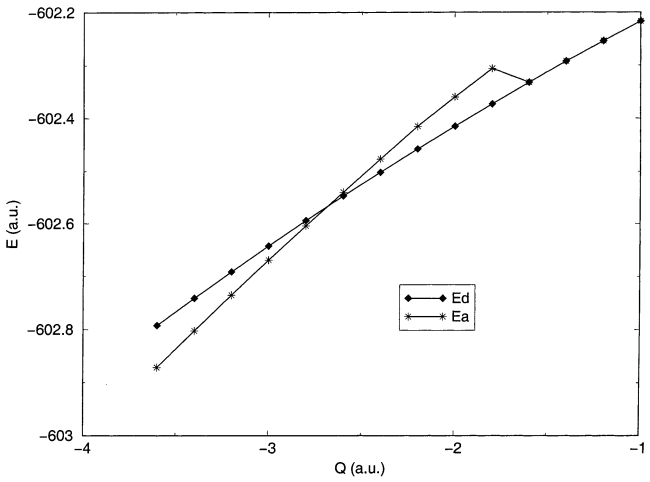


**Figure 1.** In the charge transfer system, $(His)_2(Met)Cu(I/II)$-$(Cys)$-$(Gly)_5$-$(His)Ru(III/II)(bpy_2)Im$ donor and acceptor state energies near the resonance charge $Q = 2.6893$ au region and at the far-end region where the acceptor state collapses into the donor state at $Q = 1.6$ au.

One remark is needed on how to obtain two states for a given charge $Q$. In ZINDO, like in other variational HF calculations, the SCF procedure yields a state that corresponds to a local minimum of the energy functional. A different choice of the initial orbitals may result in different converged states. Typically, in ET calculations, there are two strongly attracting minima, provided that the energies of two states are similar. The calculations are performed starting from some value of the external charge, say $Q = 0$, and the convergence is obtained for an arbitrary state, which most likely is the ground state of the system. The external charge then is varied by a small amount in such a way as to force the rearrangement of the electrons in the system that would correspond to the other redox state. The calculation of the WF for a new charge begins from the trial state obtained from the previous calculation. The convergence in this case occurs to the same local minimum in energy space as for the previous calculation, provided the changes are small. Thus, gradually changing the charge, the variational calculation will eventually yield an excited state. (Rigorously speaking, neither of the two states is exactly ground or first excited state. This description is only valid within the context of variational SCF calculations.) Such calculations continue until the charge has changed to such an extent that a different minimum of much lower energy has developed, and the convergence results in a new state of lower energy—the ground state, with rearranged electrons that correspond to the second redox state of the system. Now taking the new set of orbitals, the calculation proceeds with a gradual variation of charge in the opposite direction, until the first state is recovered. The calculations result in two functions, $E_d(Q)$ and $E_a(Q)$, that cross at some pont $Q\dagger$. The exact value of $Q\dagger$ is determined by the extrapolation method, as mentioned above (Figure 1).

## 3. Results and Discussion

In obtaining the numerical results in this section, the donor and acceptor states are all calculated at the open shell unrestricted HF(UHF) level of theory using a single Slater determinant and, except for ab initio calculations, with minimum basis set. As in most electronic structure calculations using INDO theory, core orbitals are frozen; therefore, they do not explicitly contribute to the valence orbital wavefuntion nor to the tunneling current density. The choices of the semiempirical ZINDO/S model is standard as in ref 50. Unless specified

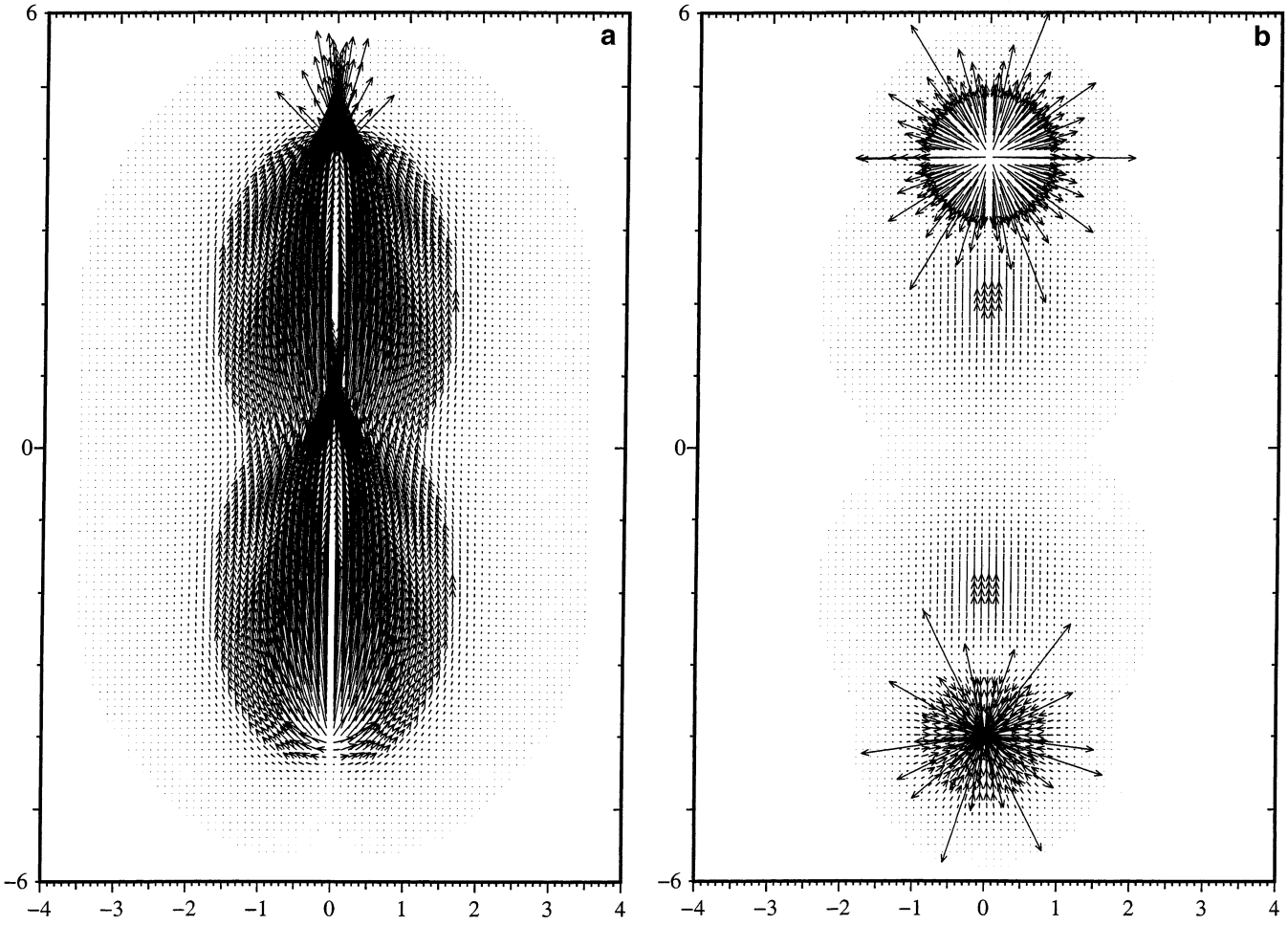


**Figure 2.** (a) $H_3^+$ linear system current density from this model calculation. (b) $H_3^+$ linear system current density from Gaussian calculation.

otherwise, all of the computations in this section are carried out by using the algorithm and programs developed in STO basis sets[51] in connection with the ZINDO electronic structure package.[52]

**3.1. STO vs GTO.** Before we discuss an application of the ZINDO model to a complex redox system, here, we would like to illustrate a simple but an important point regarding the choice of the atomic basis functions in tunneling calculations.

As is well-known, the framework of ZINDO basis set is STO atomic functions, while ab initio calculations are based on GTO. The incorrect behavior of GTO at large distances forces the use of several Gaussian functions to improve the asymptotic behavior of the resulting atomic functions, a practice commonly referred to as STO-*n*G, with *n* usually being 3 or 6. In practice, any finite number of Gaussian primitives can provide a correct approximation only within a small range of distances typically limited to lengths of chemical bonds. In tunneling calculations, however, the small interactions of atoms at large distances, which are unimportant in standard quantum chemistry calculations, can make a big difference. In particular, a cumulative effect of a large number of small interactions can be significant.[34]

Obviously, the correct asymptotic behavior of the STO makes these functions particularly useful for tunneling calculations in systems such as proteins. One does not need to use a large number of diffusive functions to account for nonchemical "through space"[53] interactions. A minimum STO basis set with correctly optimized exponentials is usually sufficient.

To illustrate this point, in Figure 2, the tunneling currents are shown for a model system $HHH^+$ calculated with both GTO and STO. The interatomic distance is set to be 4 Å. An electric field with the strength of 0.02 au is applied to break the symmetry of the system and to localize the electron on the end sites of the chain.

The results of ZINDO and ab initio calculations are markedly different, as shown in Figure 2a,b. The ab initio calculation is carried out with Dunning/Huzinaga full double $\zeta$ basis set using Gaussian 94.[54] A discontinuous current flow exists in the midchain of $H_3^+$ in the ab initio results. A close examination of tunneling flux shows a steady average value of 0.1398 $cm^{-1}$ in ZINDO results while the ab initio results fluctuate between $\pm 9.2$ $cm^{-1}$ with change of signs at 3 Å and $-3$ Å along the molecular axis.

It is obvious that in this simple case the Gaussian calculation is unable to correctly produce steady tunneling current and electronic coupling through 4 Å of space separating the adjacent hydrogen atoms. This problem with long-distance behavior of the GTO basis functions is expected to cause serious defects in calculations of electron transfer in biological systems where hydrogen bonds and through space tunneling, both at lengths significantly larger than the conventional chemical bonding distance, may be important.

**3.2. The Polypeptide $(His)_2(Met)Cu^{1+}$-(Cys)-$(Gly_5)$-(His)-$Ru^{3+}(bpy_2)$Im System.** This system, shown Figure 3, is a model for a tunneling pathway in Ru-modified protein Azurin studied by Gray and co-workers.[55] Here, a single polypeptide chain

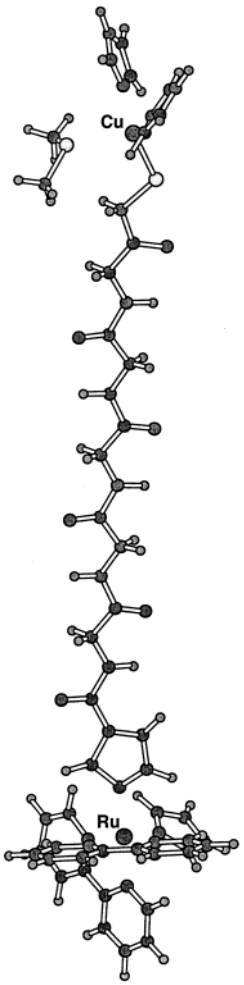


**Figure 3.** $(His)_2(Met)Cu(I/II)$-(Cys)-$(Gly_5)$-(His)Ru(III/II)$(bpy_2)$Im charge transfer system.

bridges two transition metal complexes, between which electron tunneling occurs. In the experimental studies, the Ru complex is initially in the reduced (2+) form. The short laser pulse initiates the charge transfer reaction by ionizing the Ru complex and making it $Ru^{3+}$. The transient kinetics then follows in which Ru complex is reduced, and simultaneously, the copper complex is oxidized. Electron donors and acceptors in the calculations are Cu(I) of the blue copper center in the reduced form and the $Ru^{3+}$ ion in $-HisRu^{3+}(bpy_2)Im$ complex. The donor and acceptor complexes are coordinated to the opposite ends of the polypeptide $(Gly)_5$ chain, similar to the system studied earlier.[22]

Because the two ends of the polypeptide chain are not equivalent, the diabatic states, D-bridge-$A^+$ and $D^+$-bridge-A, have different energies, $E_d$ and $E_a$; therefore, no charge transfer can occur. ($E_d$ and $E_a$ are total electronic energies of the system.) To induce the charge transfer, the two states need to be brought into resonance. In the absence of polar thermal fluctuations of a media, our calculation places a point charge $Q$ exactly 8 Å above the Ru atom along the pseudo-axis of the system. With the method described in the previous section, the computed $E_d$ and $E_a$ near resonances are shown in Figure 1. A least-squares procedure determines the resonance charge $Q$†, which happened to be 2.689 au, at which $\Delta E_{da} = E_a - E_d = 10\ cm^{-1}$. The donor and acceptor states calculated at this value of the external charge are then used in tunneling calculations. (Formally, the two state energies $E_a$ and $E_d$ should be in exact resonance or within the splitting distance, $|T_{DA}|$, from each other. In practice, however, the distances $\Delta E_{ad}$ of $10-100\ cm^{-1}$, depending on the value of $T_{DA}$, are typically found to be satisfactory. We check the consistency of calculations of $T_{DA}$ by varying $\Delta E_{ab}$ and accepting the converged value of $T_{DA}$, as the resonance condition is improved; see further discussion of this issue in ref 15.)

The two states are first biorthogonalized, and tunneling orbitals are examined qualitatively. Two features of the donor and acceptor sites are perhaps worth noting here. One is that the tunneling electron seems to predominantly involve the sulfur bonded to the blue copper instead of the copper itself, an indication that $S$ is quite "metallic" as in nanoswitches.[56] The other observation in this calculation is that the acceptor state does not rest on the three bipyridines equally; it has dominant contribution from the one nearest to the Ru atom, confirming an ultrafast dynamics experiment on photoinduced charge transfer.[57] Of greater interest is the comparison to make below with the ab initio calculations because this system is the largest system that the ab initio method has been applied on to date.[22]

The features of the current density, eq 8, and total flux, eq 4, shown in Figures 4 and 5, respectively, by and large confirm the results of ab initio calculations.[22] Notably, the wavy periodic structure of the total flux, Figure 5, which arises due to the irregularities in spatial behavior of the MOs composed of a finite number of atomic functions, is more pronounced and regular in this work. The stationary, although periodically varying, behavior of the flux is the signature of the correctness of calculations. The amplitude of variations of the flux can be used for an estimate of the error bars on our calculations (for given parametrization of the ZINDO).

With the unadjusted ZINDO parameters, the average total flux is $3.8 \times 10^{-5}\ cm^{-1}$, which is about 1 order of magnitude smaller than the ab initio result obtained earlier for the same system.[22] There are two possible sources of this difference. One is the weakening of the two state interaction due to applied ZDO approximation. To examine this effect, we computed total flux with Löwdin type orbitals (LTO)[58] and found a near-constant ratio of 1.5 of the LTO over ZDO fluxes. This factor prompts that ZDO is perhaps a little too severe, and a small correction factor introduced into empirical overlap integrals of ZINDO would bring results closer to ab initio calculations. Indeed, an additional factor of $f = 1.02$ in the overlap integrals results in an average total flux of $5.4 \times 10^{-4} cm^{-1}$, which compares well with the ab initio result.[22] This factor would not significantly affect the energy predictions made by the program. Thus, a "weak reparametrization" could be applied to "tune" ZINDO for tunneling calculations. In the absence of reliable direct experimental data on the tunneling matrix elements, however, such a reparametrization is difficult to rely upon.

The other source of discrepancy is the way how the two approaches treat the metal complexes, i.e., the core part of the tunneling orbitals. The ab initio HF calculation is known to be inaccurate in describing charge distribution between the metal and the ligand atoms. On the other hand, ZINDO is based on experimental data for such complexes and therefore is expected to be more reliable in this regard. Yet, in the absence of direct experimental data for $T_{DA}$, it is difficult to make solid conclusions. The evaluation of the absolute value of such a subtle quantity as a small tunneling matrix element in such complex systems as proteins remains a challenging problem.

The distance dependence of matrix element from this calculation is carried out by truncating glycines successively to reduce the polypeptide charge transfer bridge length. The results as shown in Figure 6 produce the expected linear relation of $\log|T_{DA}|^2$ over charge transfer distance. It is noticible that both the ab initio and the ZINDO calculations give the same slope,

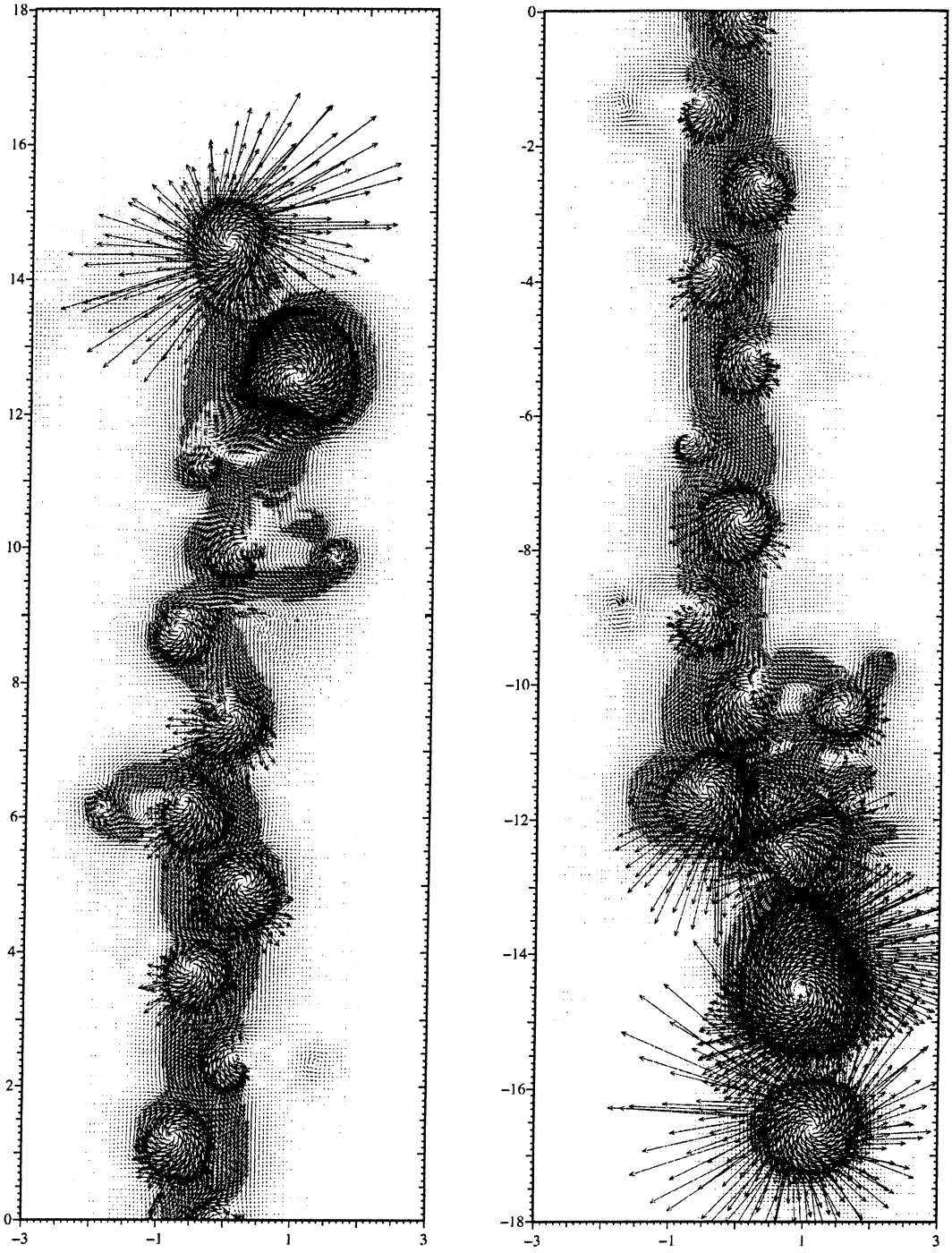


**Figure 4.** Calculated current density of the charge transfer system $(His)_2(Met)Cu(I/II)$-(Cys)-$(Gly)_5$-(His)$Ru(III/II)(bpy_2)Im$ in this work.

which coincides with that observed in experiments.[59] The same slope probably means that the reparametrization of overlaps is not a good idea, and the main source of discrepancy in absolute value is in the way how the metal complexes are treated by two models.

Our final consideration in these calculations is to examine the tails of the tunneling orbitals. As discussed in section 2, the tunneling calculations deal with wave functions that extend far under the tunneling barrier between the donor and the acceptor sites into the protein medium. One concern in such calculations has always been how accurately the variational calculations of donor and acceptor states, which are designed to optimize the total energy of the system, can describe the small tunneling tails of the wave functions. Moreover, by their nature, the diabatic states are not well-defined in the very far end of the tail region that correspond to the other redox site. To examine the quality of our waver functions, we calculated atomic populations by converging the HF equation to one part in $10^{-4}$ (loose convergence), $10^{-6}$ (normal convergence), and $10^{-12}$ (tight convergence) in energy, respectively. Figure 7a,b gives the results for C and N atoms, which lie directly in the electron tunneling pathway. It is seen in these figures that the population is smoothly (exponentially) decreasing with distance along the pathway; however, the far tail of the wave functions is very irregular. The tunneling currents method uses the barrier part of the wave functions only, where both donor and acceptor

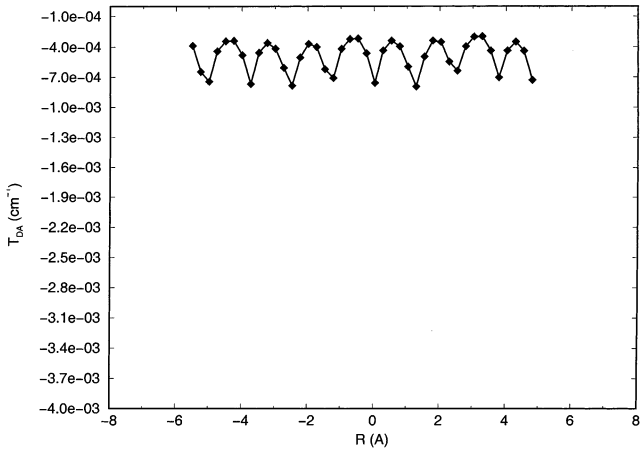


**Figure 5.** Calculated total flux (matrix element) of the tunneling current of the charge transfer system $(His)_2(Met)Cu(I/II)$-(Cys)-$(Gly)_5$-(His)-$Ru(III/II)(bpy_2)Im$ in this work. $f_t$ is set to 1.0 (unadjusted model).

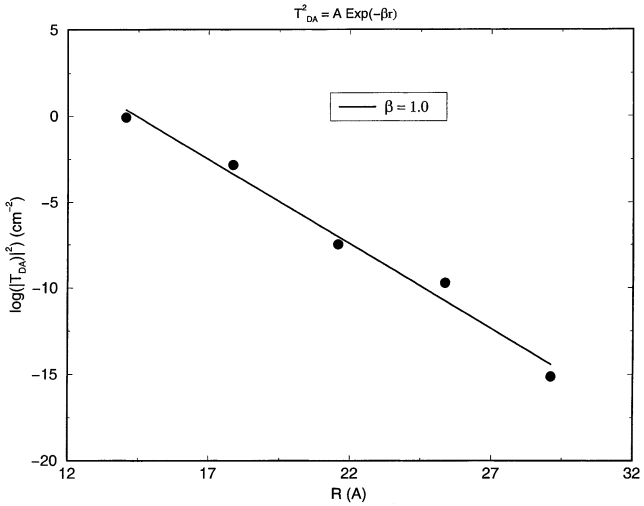


**Figure 6.** Distance dependence of the tunneling matrix elment.

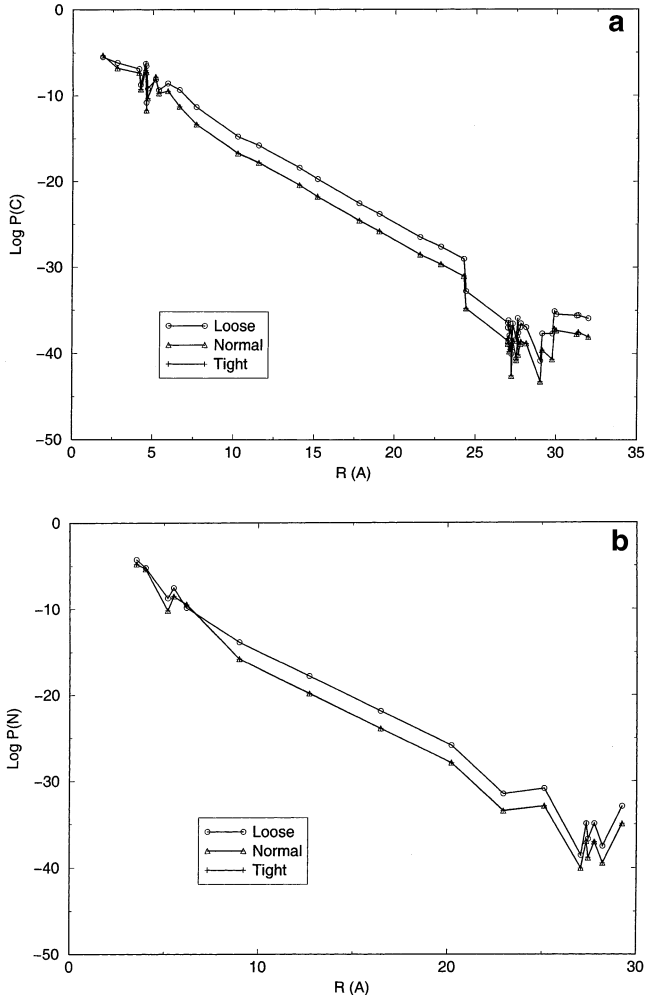


**Figure 7.** (a) Carbon atomic orbital population of the donor tunneling orbital over the distance from the cysteine sulfur. (b) Nitrogen atomic orbital population of the donor tunneling orbital over the distance from the cysteine sulfur.

tunneling orbitals are well-defined. The convergence criteria are an important issue; however, it is seen that even for this large system, the usual variational calculations of the tunneling orbitals with tight convergence are realistic and reliable.

## 4. Conclusion

The tunneling currents method has been implemented using the ZINDO model of electronic structure of the medium in which tunneling occurs. Employing Slater type orbitals, single $\zeta$ minimum basis set valence electrons only calculations in this study compare well with the sophisticated ab initio calculations in obtaining basic features of current density and total flux. In the case of our model polypeptide system, our average total flux is about 1 order of magnitude smaller than that of the ab initio calculation. The slope of the distance dependence is the same as in ab initio calculations. The discrepancy is most likely related to the way both methods treat the transition metal complexes.

By computing the atomic populations, the tunneling orbital's tails have been examined. A well-behaved exponential dependence is observed for atoms directly lying along the tunneling path in the middle part of the barrier, the part that is used for tunneling matrix element calculations. The behavior of the far tail of the diabatic states, in contrast, is unstable. In most applications, an UHF calculation converged to one part of $10^{-6}$ in energy is sufficient for a reliable calculation of the tunneling tails of the wave functions.

This implementation of the tunneling current theory bridges the gap between simple one electron methods and sophisticated ab initio methods and retains the basic features of the ZINDO model—efficiency and accuracy. The current method is particularly suitable for studies involving extended charge transfer systems in biology. Computations based on the method in this work are being carried out to investigate electron transfer pathways of some metalloprotein systems of considerable interest in both theory and experiment.[60]

**Acknowledgment.** We thank Dr. Jongseob Kim (Polytech University, Korea) for peptide model geometries, Dr. Yuri Georgievski for insights on tunneling orbital methods, and Dima Medvedev for computing assistance. Preliminary results of this study were presented at the Zerner memorial symposium at the Quantum Theory Project (QTP) of the University of Florida. We thank Professor Martin Gouterman (University of Washington), Dr. Marshall Newton (Brookhaven National Laboratory), and Professor Sven Larsson (Chalmers University of Technology) for stimulating discussions. Professor John Head (University of Hawaii) provided valuable perspectives on ZINDO. This work was supported by the ACS PRF and by the National Science Foundation.

## References and Notes


(1) Gray, H. B.; Winkler, J. R. *Annu. Rev. Biochem.* **1996**, *110*, 8865.
(2) Moser, C. C.; Keske, J. M.; Warncke, K.; Farid, R. S.; Dutton, P. L. *Nature* **1992**, *355*, 796.
(3) Page, C. C.; Moser, C. C.; Chen, X.; Dutton, P. L. *Nature* **1999**, *402*, 47.
(4) Eggers, E.; Michel-Beyerle, M. E.; Giese, B. *J. Am. Chem. Soc.* **1998**, *120*, 12950.
(5) Giese, B. *Acc. Chem. Res.* **2000**, *33*, 631.
(6) Ratner, M. *Nature* **1999**, *397*, 480.
(7) Mujica, V.; Nitzan, A.; Mao, Y.; Davis, W.; Kemp, M.; Roitberg, A. E.; Ratner, M. *Adv. Chem. Phys.* **1999**, *107*, 403.
(8) Skourtis, S. S.; Beratan, D. *Adv. Chem. Phys.* **1999**, *106*, 377.
(9) Regan, J. J.; Onuchic, J. N. *Adv. Chem. Phys.* **1999**, *107*, 497.
(10) Balabin, I. A.; Onuchic, J. N. *Science* **2000**, *114*, 114.
(11) Newton, M. D. *Chem. Rev.* **1991**, *91*, 767.
(12) Newton, M. D. *Adv. Chem. Phys.* **1999**, *106*, 303.
(13) Newton, M. D. *Int. J. Quantum Chem.* **2000**, *77*, 255.
(14) Bixon, M.; Jortner, J. *Adv. Chem. Phys.* **1999**, *106*, 107.
(15) Stuchebrukhov, A. A. *Adv. Chem. Phys.* **2001**, *118*, 1.
(16) Stuchebrukhov, A. A. *Int. J. Quantum Chem.* **2000**, *77*, 16.
(17) Stuchebrukhov, A. A. *J. Chem. Phys.* **1996**, *104*, 8424; **1996**, *105*, 10819; **1997**, *107*, 6495; **1998**, *108*, 8499.
(18) Daizadeh, I.; Medvedev, D. M.; Stuchebrukhov, A. A. *Mol. Biol. Evol.* **2002**, *19*, 987.
(19) Medvedev, I. D. D. M.; Stuchebrukhov, A. A. *J. Am. Chem. Soc.* **2000**, *122*, 6571.
(20) Medvedev, D.; Stuchebrukhov, A. A. *J. Theor. Bio.* **2001**, *210*, 237.
(21) Gehlen, J. N.; Daizadeh, I.; Stuchebrukhov, A. A.; Marcus, R. A. *Inorg. Chim. Acta* **1996**, *243*, 271.
(22) Kim, J.; Stuchebrukhov, A. A. *J. Phys. Chem.* **2000**, *104*, 8606.
(23) Wang, J.; Stuchebrukhov, A. A. *Int. J. Quantum Chem.* **2000**, *80*, 591.
(24) Pople, J. A.; Beveridge, D. L.; Dobosh, P. A. *J. Chem. Phys.* **1967**, *47*, 2026.
(25) Ridley, J.; Zerner, M. C. *Theor. Chim. Acta* **1973**, *32*, 111.
(26) Cory, M. G.; Kostlmeier, S.; Kotzian, M.; Rosch, N.; Zerner, M. C. *J. Chem. Phys.* **1994**, *100*, 1353.
(27) Kurnikov, I. V.; Beratan, D. N. *J. Chem. Phys.* **1996**, *105*, 9561.
(28) Loew, G. *Int. J. Quantum Chem.* **2000**, *77*, 54.
(29) Scherer, P. O. J.; Fisher, S. *Chem. Phys.* **1989**, *131*, 115.
(30) Thompson, M. A.; Fajer, J.; Zerner, M. C. *J. Phys. Chem.* **1991**, *95*, 5693.
(31) Cory, M. G.; Zerner, M. C.; Hu, X. H.; Schulten, K. *J. Phys. Chem.* **1998**, *102*, 7640.
(32) Newton, M. D. *J. Phys. Chem.* **1988**, *92*, 3049.
(33) Miller, N. E.; Wander, M. C.; Cave, R. J. *J. Phys. Chem. A* **1999**, *103* (8), 1084.
(34) Castner, E. W.; Kennedy, D.; Cave, R. J. *J. Phys. Chem. A* **2000**, *104* (13), 2869.
(35) Cave, R. J.; Newton, M. D. *J. Chem. Phys.* **1997**, *106* (22), 9213.
(36) Marcus, R. A.; Sutin, N. *Biochim. Biophys. Acta* **1985**, *811*, 265.
(37) Daizadeh, I.; Medvedev, E. S.; Stuchebrukhov, A. A. *Proc. Natl. Acad. Sci. U.S.A.* **1997**, *94*, 3703.
(38) Brooks, C. L.; Onuchic, J. N.; Wales, D. J. *Science* **20001**, *293*, 612.
(39) Miller, W. H.; Schartz, S. D.; Tromp, J. W. *J. Chem. Phys.* **1983**, *79*, 4889.
(40) Truhlar, D. G.; Garret, B. C. *Annu. Rev. Phys. Chem.* **1984**, *35*, 159.
(41) Harriman, J. *J. Chem. Phys.* **1964**, *40*, 2827.
(42) Amos, A. T.; Hall, G. G. *Proc. R. Soc. (London)* **1961**, *A263*, 483.
(43) Amos, A. T.; Hall, G. G. *Proc. R. Soc. (London)* **1961**, *A263*, 483.
(44) King, H.; Stanton, R. E.; Kim, H.; Wyatt, R. E.; Parr, R. G. *J. Chem. Phys.* **1967**, *47*, 1936.
(45) Voter, A. F.; Goddard, I. W. A. *Chem. Phys.* **1981**, *57*, 253.
(46) Hardisson, A.; Harriman, J. *J. Chem. Phys.* **1967**, *46*, 3639.
(47) Cory, M. G.; Zerner, M. C. *J. Phys. Chem.* **1999**, *36*, 7287.
(48) Zhang, L. Y.; Murphy, R.; Friesner, R. A. *Ab Initio Quantum Chemical Calculation of Electron Transfer Matrix Element for Large Molecules*; Schrodinger, Inc.: Portland, OR, 1997.
(49) Newton, M. D.; Ohta, K.; Zhong, E. *J. Phys. Chem.* **1991**, *95*, 2317.
(50) Zerner, M. C. *Rev. Comput. Chem.* **1991**, *2*, 313.
(51) Zheng, X.; Zerner, M. C. *Int. J. Quantum Chem.* **1993**, *S27*, 431.
(52) Zerner, M. C.; Ridely, J. E.; Bacon, A.; McKelvey, J.; Edwards, W.; Head, J. D.; Culberson, C.; Cory, M. G.; Zheng, X.; Parkinson, W.; Yu, Y.; Cameron, A.; Tamm, T.; Pearl, G.; Broo, A.; Albert, K.; et al. *ZINDO*; Quantum Theory Project, the University of Florida, Gainesville, FL 32611, distributed by Accelrys Inc.: San Diego, CA, 2001.
(53) Onuchic, J. N.; Beratan, D. N.; Winkler, J. R.; Gray, H. B. *Science* **1992**, *258*, 1740.
(54) Frisch, M. J.; Trucks, G. W.; Schlegel, H. B.; Gill, P. M. W.; Johnson, B. G.; Robb, M. A.; Cheeseman, J. R.; Keith, T.; Petersson, G. A.; Montgomery, J. A.; Raghavachari, K.; Al-Laham, M. A.; Zakrzewski, V. G.; Ortiz, J. V.; Foresman, J. B.; Cioslowski, J.; Stefanov, B. B.; Nanayakkara, A.; Challacombe, M.; Peng, C. Y.; Ayala, P. Y.; Chen, W.; Wong, M. W.; Andres, J. L.; Replogle, E. S.; Gomperts, R.; Martin, R. L.; Fox, D. J.; Binkley, J. S.; Defrees, D. J.; Baker, J.; Stewart, J. P.; Head-Gordon, M.; Gonzalez, C.; Pople, J. A. *Gaussian 94*, revision E.2; Gaussian, Inc.: Pittsburgh, PA, 1995.
(55) Langen, R.; Chang, I.; Germanas, J. P.; Richards, J. H.; Winkler, J. R.; Gray, H. B. *Science* **1995**, *268*, 1733.
(56) Gittins, D. I.; Bethell, D.; Schiffrin, D. J.; Nichols, R. J. *Nature* **2000**, *408*, 67.
(57) Yeh, A.; Shank, C. V.; McCusker, J. *Science* **2000**, *291*, 289.
(58) Szabo, A.; Ostlund, N. S. *Modern Quantum Chemistry*; Macmillan: New York, 1982.
(59) Casimiro, D. R.; Richards, J. H.; Winkler, J.; Gray, H. *J. Phys. Chem.* **1993**, *97*, 13073.
(60) Zheng, X.; Stuchebrukhov, A. A. *J. Phys. Chem. B*, accepted for publication.